Simulation study of the isotropic-to-nematic transitions of semiflexible polymers

Marjolein Dijkstra* and Daan Frenkel
FOM–Institute for Atomic and Molecular Physics, Kruislaan 407, 1098 SJ Amsterdam, The Netherlands
(Received 9 January 1995)

We report computer simulations of a three-dimensional system of semiflexible polymers consisting of hard spherocylinders connected by joints of variable flexibility. In these simulations, we have studied the influence of molecular flexibility on the location of the isotropic-nematic phase transition. A comparison of our numerical results with available theoretical predictions indicates that the existing theories systematically overestimate the density of the coexisting phases. We observe that our simulation data agree well with the available experimental data.

PACS number(s): 64.70.Md, 61.25.Hq, 61.20.Ja

I. INTRODUCTION

Liquid-crystalline phases of semiflexible polymers play an important role both in biological and in synthetic materials [1–3]. There is ample experimental evidence that semiflexible molecules can exhibit a rich phase behavior [4]. Prediction of the phase behavior of such polymeric materials is an important step towards a full characterization of the structural and dynamical properties of liquid-crystalline polymeric materials. The theoretical study of semiflexible polymers was initiated by Flory as early as 1956 [5]. And, although there is by now a large body of theoretical knowledge on semiflexible polymers, the statistical behavior of bulk systems of semiflexible polymers is still incompletely understood. In Flory's approach, the polymers are modeled as self-avoiding random walks on a three-dimensional lattice. The fraction of bonds that are bent in equilibrium provide a measure for the molecular flexibility. When treated at the mean-field level, the Flory model exhibits a first-order phase transition from the isotropic phase to an orientationally ordered state, when the flexibility drops below a critical value. Other mean-field theories [6–8] also predict such a phase transition for three-dimensional lattice polymers. However, these mean-field results appear to be at odds with the fact that several exactly solvable (but highly simplified) models for three-dimensional lattice polymers exhibit a continuous phase transition [9,10]. It would therefore seem that computer simulation is a logical tool to investigate the phase behavior of semiflexible polymers. In fact, several authors have reported such simulations [11,12]. However, somewhat surprisingly, long-range orientational order has thus far not been observed in such simulations of three-dimensional athermal lattice polymers. Simulations of athermal polymers on a cubic lattice [11] and on a tetrahedral lattice [12] do not show the onset of long-range orientational order, but the formation of ordered *domains*. The linear dimension of these domains is of the order of the contour length of the polymer. In Refs. [11,12], a true isotropic-nematic phase transition of semiflexible lattice polymers was only observed if an attractive interaction between parallel nearest neighbor segments was included. The reason why the athermal semiflexible polymers do not seem to form an orientationally ordered phase may, at least in part, be due to the fact that the simulations referred to above were all performed on lattice models. Also, the theoretical approaches for lattice models that are described above give conflicting predictions about the phase transition. It is therefore of considerable interest to consider an off-lattice system of continuously deformable polymers. Simulations of a specific off-lattice system of semiflexible chain molecules consisting of linked hard spheres showed the presence of three fluid phases, that were identified as isotropic, nematic, and smectic A [13]. In fact, all existing theories for the phase behavior of off-lattice models for three-dimensional semiflexible polymers predict a first-order isotropic-to-nematic phase transition [14–19]. These theories for the phase behavior of off-lattice semiflexible polymers will be reviewed in more detail in Sec. II. At this stage, it is important to note that these theories make significantly differing predictions for the phase diagram. It is therefore interesting to investigate the phase behavior of off-lattice semiflexible polymers systematically by computer simulations. In this paper, we describe Monte Carlo simulations of a three-dimensional system of semiflexible polymers consisting of hard spherocylinders connected by joints of variable flexibility. In particular, we investigate the influence of flexibility on the isotropic-nematic phase transition. The simulation method is discussed in Sec. III and the results of the simulations are reported in Sec. IV.

II. THEORIES OF THE ISOTROPIC-NEMATIC TRANSITION OF SEMIFLEXIBLE CHAINS

Let us first briefly review the theoretical predictions for the coexistence densities of the isotropic and nematic

*Present address: Physical Chemistry Laboratory, Oxford University, South Parks Road, Oxford OX1 3QZ, United Kingdom.

phases in two extreme cases, namely, for rigid rods and for wormlike chains. First, we consider a fluid of hard rods of length L and diameter D in the "Onsager" limit $L \gg D$. In that limit, the expression for the Helmholtz free energy F of the fluid consisting of N particles reads

$$\frac{F}{Nk_BT} = \log(\Lambda^3\rho) - 1 + \sigma^{(0)}_{\text{rigid}} + B_2\rho, \tag{1}$$

with

$$\sigma^{(0)}_{\text{rigid}} = \int f(\Omega)\log(4\pi f(\Omega))d\Omega, \tag{2}$$

$$B_2 = L^2D\int f(\Omega)f(\Omega')|\sin\gamma|d\Omega d\Omega', \tag{3}$$

where Λ is the de Broglie thermal wavelength. For a given density ρ the free energy must be minimized with respect to the orientational distribution function $f(\Omega)$. At low densities, the only possible solution is $f(\Omega) = f_{\text{iso}}(\Omega) = 1/4\pi$, representing the isotropic phase. In that case, the contribution to the free energy due to the orientational entropy $\int f_{\text{iso}}(\Omega)\log(4\pi f_{\text{iso}}(\Omega))d\Omega$ vanishes. The contribution due to the translational entropy becomes $\rho\pi DL^2/4$. At sufficiently high densities, a second solution of the minimum condition is possible, representing the nematic phase, with $f(\Omega) = f_{\text{nem}}(\Omega)$. The exact functional form of $f_{\text{nem}}(\Omega)$ is unknown, but several approximations, which will be discussed below, have been proposed in the literature. Because of the first-order character of the isotropic-nematic transition, there is a density regime, where an isotropic phase of density ρ_{iso} coexists with a nematic phase of density ρ_{nem} and orientational distribution function $f_{\text{nem}}(\Omega)$. The coexisting phases must be in thermal, mechanical and chemical equilibrium, implying that the temperature T, the osmotic pressure Π, and the chemical potential μ are the same in both phases:

$$\begin{aligned} T_{\text{iso}} &= T_{\text{nem}}, \\ \Pi_{\text{iso}}(\rho_{\text{iso}}) &= \Pi_{\text{nem}}(\rho_{\text{nem}}), \\ \mu_{\text{iso}}(\rho_{\text{iso}}) &= \mu_{\text{nem}}(\rho_{\text{nem}}). \end{aligned} \tag{4}$$

The osmotic pressure and chemical potential are easily obtained by the thermodynamic relations

$$\Pi(\rho) = -\left(\frac{\partial F}{\partial V}\right)_{N,T}, \tag{5}$$

$$\mu(\rho) = \left(\frac{\partial F}{\partial N}\right)_{V,T}. \tag{6}$$

Note that $\mu_{\text{nem}}(\rho_{\text{nem}})$ and $\Pi_{\text{nem}}(\rho_{\text{nem}})$ depend functionally on $f_{\text{nem}}(\Omega)$. The conditions in Eq. (4) and the extremum condition of the Helmholtz free energy are sufficient to determine (numerically) the values for ρ_{iso}, ρ_{nem}, and $f_{\text{nem}}(\Omega)$. One way of doing this is to approximate $f_{\text{nem}}(\Omega)$ by a trial function of one or more variational parameters. A particularly simple trial function is the Gaussian distribution [16]

$$f(\theta) = \begin{cases} (\alpha/4\pi)\exp\left[-\alpha\theta^2/2\right], & 0 \le \theta \le \pi/2 \\ (\alpha/4\pi)\exp\left[-\alpha(\pi-\theta)^2/2\right], & \pi/2 \le \theta \le \pi, \end{cases} \tag{7}$$

where α is the variational parameter. Introducing the reduced density $c \equiv \rho\nu_0 L/D = \phi L/D$, where ϕ is the volume fraction of the rods and ν_0 the volume of one rod, the Gaussian approximation leads to [16]

$$c_{\text{iso}} = 3.45, \quad c_{\text{nem}} = 5.12, \quad \alpha = 33.4. \tag{8}$$

However, if instead we use the trial function suggested by Onsager,

$$f(\cos\theta) = \frac{\alpha\cosh(\alpha\cos\theta)}{4\pi\sinh\alpha}, \tag{9}$$

we obtain the following results [20]:

$$c_{\text{iso}} = 3.340, \quad c_{\text{nem}} = 4.486, \quad \alpha = 18.58. \tag{10}$$

Not surprisingly, the prediction for the coexisting concentrations depends somewhat on the precise form chosen for the trial function.

Although Eq. (4) cannot be solved analytically, it is possible to find the solution numerically. This approach was pioneered by Lasher [21] and subsequently refined by Kayser and Raveché [22], by Lekkerkerker *et al.* [23] and by Herzfeld, Berger, and Wingate [24]. Using this method, Lekkerkerker *et al.* and Herzfeld, Berger, and Wingate obtained the following result [23,24]:

$$c_{\text{iso}} = 3.290, \quad c_{\text{nem}} = 4.191. \tag{11}$$

The difference between this "exact" result and the approximate answers given by Eqs. (8) and (10) is due to the choice of the approximate trial functions. The Onsager trial function and the Gaussian trial function are too sharply peaked and, consequently, the contribution to the free energy due to the orientational entropy is overestimated and that due to the translational entropy is underestimated. The overestimate of the total Helmholtz free energy of the nematic phase decreases with increasing density. As a result, the tendency to form the nematic phase is postponed to higher concentrations in the case of these trial functions.

Next, we consider the predictions for the phase-coexistence densities in systems of semiflexible rods of contour length L, diameter D, and persistence length l_P. The Onsager rigid-rod model that we discussed above can be considered a limiting case of semiflexible rods for $l_P \gg L \gg D$. Below, we briefly review the wormlike chain limit $L \gg l_P \gg D$. The coexistence densities of polymers with arbitrary flexibility may be estimated by interpolation between the Onsager and the wormlike-chain limit.

Khokhlov and Semenov [14,15], derived the following expression for the Helmholtz free energy for semiflexible polymers in the limit $L \gg l_P \gg D$. This limit describes the case of chains that are locally very stiff, but are so long that they can still form coils:

$$\frac{F}{Nk_BT} = \log(\Lambda^3\rho) - 1 + \sigma(f) + B_2\rho \tag{12}$$

where

$$\sigma(f) = -\frac{L}{2l_P}\int f^{1/2}(\Omega)\Delta f^{1/2}(\Omega)d\Omega$$

with $f(\Omega)$ the segment orientation distribution function and Δ the Laplacian. Again, in the isotropic phase the orientational entropy $\sigma(f)$ is zero and the contribution to the free energy due to the translational entropy is given by $B_2\rho = \rho\pi DL^2/4$. If we now use again a Gaussian trial function for the orientational distribution function for the segments, we obtain the following coexistence concentrations (in reduced units $c^* \equiv \phi\, l_P/D$) [4]:

$$c^*_{\rm iso} = 7.77, \quad c^*_{\rm nem} = 9.71, \quad \alpha = 12.34. \tag{13}$$

The Onsager trial function gives the following results [16]:

$$c^*_{\rm iso} = 5.409, \quad c^*_{\rm nem} = 6.197, \quad \alpha = 6.502. \tag{14}$$

The numerical minimization of Eq. (12) [25] yields

$$c^*_{\rm iso} = 5.124, \quad c^*_{\rm nem} = 5.509. \tag{15}$$

Thus far we have only discussed the coexisting concentrations for two extreme cases, namely, the rigid-rod limit and the very long coil limit. In practice, one is usually interested in systems that are situated between these two limits. Khokhlov and Semenov calculated the correction terms to the orientational free energy $\sigma(f)$ near the rigid-rod and wormlike-chain limits [15].
For $L \ll l_P$,

$$\begin{aligned}\sigma(f) &= \sigma^{(0)}_{\rm rigid}(f) + \sigma^{(1)}_{\rm rigid}(f) \\ &= \int f(\Omega)\log[4\pi f(\Omega)]d\Omega \\ &\quad + \frac{L}{12 l_P}\int d\Omega\,(\nabla f(\Omega))^2/f(\Omega)\end{aligned} \tag{16}$$

and for $L \gg l_P$,

$$\begin{aligned}\sigma(f) &= \frac{L}{l_P}\sigma^{(0)}_{\rm worm}(f) + \sigma^{(1)}_{\rm worm}(f) \\ &= \frac{L}{8 l_P}\int d\Omega\,(\nabla f(\Omega))^2/f(\Omega) \\ &\quad -2\log\int [f(\Omega)]^{1/2}d\Omega.\end{aligned} \tag{17}$$

These expressions can be worked out further for the specific choice of the Onsager trial function [16],

$$\sigma(\alpha) = \begin{cases} \frac{L(\alpha-1)}{4 l_P} + \log(\frac{1}{4\alpha}) (L \gg l_P), & (18) \\ \log\alpha - 1 + \frac{L(\alpha-1)}{6 l_P} (L \ll l_P). & (19)\end{cases}$$

This results in the following predictions for the dependence of the coexistence density on l_P [16]:

$$c^*_{\rm iso} = 5.409 + 1.910 N_{l_P}^{-1}, \quad c^*_{\rm nem} = 6.197 + 1.781 N_{l_P}^{-1}$$

$$(N_{l_P} \gg 1), \tag{20}$$

$$c^*_{\rm iso} = 3.340 N_{l_P}^{-1} + 4.99, \quad c^*_{\rm nem} = 4.486 N_{l_P}^{-1} - 1.458$$

$$(N_{l_P} \ll 1), \tag{21}$$

where $N_{l_P} \equiv L/l_P$. In order to obtain a formula valid for arbitrary L/l_P these results can be interpolated in the form of a Padé approximant [15,16]:

$$\begin{aligned} c^*_{\rm iso} &= \frac{3.34 + 5.97 N_{l_P} + 1.585 N_{l_P}^2}{N_{l_P}(1 + 0.293 N_{l_P})}, \\ c^*_{\rm nem} &= \frac{4.486 + 11.24 N_{l_P} + 17.54 N_{l_P}^2}{N_{l_P}(1 + 2.83 N_{l_P})}. \end{aligned} \tag{22}$$

Another approach was taken by Odijk. Within the Gaussian approximation, he derived a closed expression for the orientational free energy for arbitrary chain length [16],

$$\begin{aligned}\sigma(\alpha) \simeq \log\alpha &+ \frac{\alpha-1}{6}N_{l_P} \\ &+ \frac{5}{12}\log\left(\cosh\left(\frac{\alpha-1}{5}N_{l_P}\right)\right) - \frac{19}{12}\log 2.\end{aligned} \tag{23}$$

In fact, this expression is a highly accurate approximation of the exact expression, but is easier to use in calculations. The coexisting concentrations calculated from Eq. (23) deviate significantly from the concentrations given by Eq. (22).

Hentschke proposed a semiempirical expression for the free energy of semiflexible polymers of arbitrary chain length by interpolating the orientational free energy between the rod limit and the semiflexible limit [17]:

$$\sigma_h(f) \simeq \frac{\sigma^{(0)}_{\rm rigid}(f) + \sigma_1(f) N_{l_P} + s(f)\sigma^{(0)}_{\rm worm}(f) N_{l_P}^2}{1 + s(f) N_{l_P}}, \tag{24}$$

where

$$\begin{aligned}\sigma_1(f) &= s(f)\sigma^{(0)}_{\rm rigid}(f) + \sigma^{(1)}_{\rm rigid}(f), \\ s(f) &= \frac{\sigma^{(0)}_{\rm worm}(f) - \sigma^{(1)}_{\rm rigid}(f)}{\sigma^{(0)}_{\rm rigid}(f) - \sigma^{(1)}_{\rm worm}(f)}.\end{aligned} \tag{25}$$

If we now use the Onsager trial function and retain only the leading-order terms, we find

$$\sigma_h(f) \simeq \frac{12(\log 4 - 1)(\log\alpha - 1) + (\log 16\alpha - 3)z + (1/4)z^2}{12(\log 4 - 1) + z} \tag{26}$$

where z equals $(\alpha - 1)N_{l_P}$. In addition, Hentschke used a generalization of the Carnahan-Starling equation for hard spheres to the case of spherocylinders instead of the Onsager or second virial approximation [26]. The Helmholtz free energy expression for semiflexible polymers now reads

$$\begin{aligned}\frac{F}{N k_B T} &= \log(\Lambda^3\rho) - 1 + \sigma_h(f) + A(\phi, x) \\ &\quad + B(\phi, x)\frac{4}{\pi}\int f(\Omega) f(\Omega')|\sin\gamma| d\Omega d\Omega',\end{aligned} \tag{27}$$

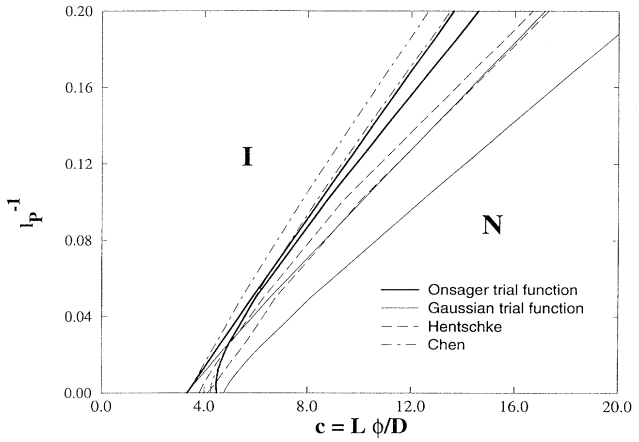

FIG. 1. Phase diagrams of a three-dimensional system of semiflexible polymers based on some of the theories mentioned in the text.

where we define $x = L/D$ and

$$A(\phi, x) = 4\phi \frac{1 - 3\phi/4}{(1-\phi)^2},$$

$$B(\phi, x) = \phi \frac{1 - 3\phi/4}{(1-\phi)^2} \frac{3x^2/2}{1 + 3x/2}. \tag{28}$$

Using this expression for the Helmholtz free energy and Onsager's trial function, Hentschke computed the phase diagram for persistent flexible hard rods [17,18]. Finally, Chen computed numerically the the isotropic-nematic coexistence densities for arbitrary L/l_P [19] (but still under the restriction $\{L, l_P\} \gg D$). Chen used a similar procedure that Herzfeld, Berger, and Wingate [24] used for studying the isotropic-nematic phase transition of rigid rods. In Fig. 1, we show that the phase diagrams computed on the basis of the several theories differ significantly from each other. A further detailed analysis of this isotropic-nematic phase transition is therefore needed.

III. MODEL AND COMPUTATIONAL TECHNIQUE

We performed computer simulations of a three-dimensional system of semiflexible polymers consisting of ten hard spherocylinders connected to each other. The ℓ/D ratio of these spherocylinders is 4, where ℓ is the segment length and D the diameter of the spherocylinder. The segment length was chosen as our unit of length. The bending energy for a joint between two segments i and $i-1$ is given by

$$u_{\hat{w}_{i-1}\hat{w}_i} = \frac{C}{2\ell}\, \theta^2_{\hat{w}_{i-1}\hat{w}_i} \tag{29}$$

where $\theta_{\hat{w}_{i-1}\hat{w}_i}$ is the angle between the unit vectors $\hat{w}_{i-1}$ and $\hat{w}_i$ that specify, respectively, the orientations of the segments $i-1$ and i and C is the elastic bending constant. We can now define a characteristic length scale on which the direction of the tangent vector along the chain alters. The so-called persistence length is directly related to the elastic bending constant C [14,15]:

$$l_P = \frac{C}{k_B T} \tag{30}$$

In the nematic phase, each polymer is strongly hindered by neighboring polymers and we can assume that each polymer is effectively confined to a tube with diameter d. The tube diameter scales with the density as $\rho^{-1/2}$. A new length scale can be introduced here, namely, the deflection length λ. The deflection length is the characteristic length scale for a semiflexible chain confined in a tube with diameter d. This length scale corresponds to the average distance between two successive deflection points of the chain in the tube and is found to scale as $\lambda \equiv l_P^{1/3} d^{2/3}$ [27,28]. Our discrete model of a semiflexible chain is only valid for polymers with a deflection length larger than the segment length. In our simulations, the deflection length was always larger than 5 in units of the segment length.

In order to compute the phase diagram, we generalized a scheme introduced by Kofke [29,30] that enables direct simulation of the phase coexistence line. This method is based on the Gibbs-Duhem equation. For our model of semiflexible polymers the Gibbs-Duhem equation reads

$$N d\mu = V dP + \left(\frac{\partial G}{\partial l_P^{-1}}\right) dl_P^{-1}, \tag{31}$$

where G is the Gibbs free energy. Using the thermodynamic conditions for coexistence of two phases [Eq. (4)], we obtain the following relation between the pressure and the persistence length l_P along the P-l_P^{-1} coexistence line:

$$\left(\frac{\partial P}{\partial l_P^{-1}}\right)_{\text{coex}} = -\frac{\Delta(\partial G/\partial l_P^{-1})}{\Delta V}, \tag{32}$$

where $\Delta(\partial G/\partial l_P^{-1})$ and ΔV denote the difference of $(\partial G/\partial l_P^{-1})$ and volume V in the coexisting phases, which can be measured easily in the simulations as

$$(\partial G/\partial l_P^{-1}) = -l_P \langle U_{\text{bend}} \rangle, \tag{33}$$

with

$$U_{\text{bend}} = \sum_{i=1}^{N} \sum_{j=2}^{k} u^i_{\hat{w}_{j-1}\hat{w}_j}$$

and k the number of segments.

Using the Kofke method [29,30], we can compute the phase coexistence curve, provided that one set of points on this curve is already known. In the present case, the known point is the limit of infinite persistence length l_P. In this limit, the semiflexible polymers reduce to hard spherocylinders. For this fully rigid limit, we performed a Gibbs ensemble Monte Carlo simulation of hard spherocylinders of length $L/D = 40$. The reduced pressure and concentrations ($c \equiv L\phi/D$) of the coexisting isotropic and nematic phase obtained from the simulations are given by

$$c_{\rm iso} = 3.075 \pm 0.015,$$
$$c_{\rm nem} = 4.065 \pm 0.015, \quad (34)$$
$$\beta\nu_0\Pi L/D = 16.36 \pm 0.88.$$

These values should be compared with the values obtained by Lekkerkerker for limit $L/D \to \infty$ [see Eq. (11)] [23]:

$$c_{\rm iso} = 3.290, \quad c_{\rm nem} = 4.191, \quad \beta\nu_0\Pi L/D = 14.116, \quad (35)$$

where the pressure of the coexisting phases is obtained by using the relation

$$\beta\nu_0\Pi L/D = c_{\rm iso} + c_{\rm iso}^2. \quad (36)$$

This expression can be obtained by minimizing the free energy for hard rods [Eq. (1)] and by using Eq. (5).

Equation (32) was solved using a four-point Adams-Bashforth-Moulton predictor-corrector algorithm (see, e.g., Ref. [31]). As such algorithms are not self-starting, we initialized the integration using a first-order predictor-corrector algorithm. Starting from $l_P^{-1} = 0$, we increased the flexibility of the polymers and computed for this new flexibility the predicted pressure. Then we performed constant pressure Monte Carlo simulations [32] at this predicted pressure for each phase and computed $\Delta(\partial G/\partial l_P^{-1})$ and ΔV, i.e., the right-hand side of Eq. (32). Using the information of the derivative at this new point obtained from the simulations, we corrected the predicted pressure. Repeating these predictor-corrector steps, we performed simulations along the $P - l_P^{-1}$ coexistence lines. After two integration steps, a second-order predictor-corrector algorithm was applied. After that, we continued with an integration routine of the fourth order.

In a constant pressure simulation, the number of particles, the pressure, and the temperature are fixed quantities. In our simulations, the number of polymers for the isotropic and the nematic phase are, respectively, 268 and 431. In the simulations, we had to ensure that no trial move would result in a hard-core overlap of the polymer segments. To test whether a trial move generated such an overlap, we used the overlap criterion for spherocylinders described in Ref. [33]. In the isothermal-isobaric Monte Carlo simulations, the following trial moves were performed:

(1) Reptation.

(2) Regrowing a whole polymer at a random position and with a random orientation using the configurational-bias Monte Carlo method (CBMC) [34].

(3) Volume changes.

Most runs consisted of at least 10^6 trial moves per polymer. Each cycle consists of, on average, one attempted reptation move per polymer and an attempt to change the volume of the box. On average, once every five reptation moves a polymer is completely regrown at a random position in the periodic box using the CBMC method. For more technical details on the regrowth of a polymer, the reader is referred to Ref. [35].

IV. RESULTS AND DISCUSSION

Using the Kofke integration scheme [29,30], we obtained the isotropic-nematic coexistence curve of a three-dimensional system of semiflexible polymers consisting of ten hard spherocylinders connected to each other. Our results are shown in Fig. 2. For the sake of comparison, we also plot the relevant theoretical predictions. We clearly observe that, compared with the theories, our simulation results for the coexisting densities are shifted systematically to lower densities. Below, we discuss the factors that are responsible for the difference between theory and computer experiment.

The first, but not the most important, reason why we find systematically lower values for the coexistence densities in our computer simulations is related to the choice of the approximate orientational distribution functions in the theoretical descriptions. In Sec. II, we have already mentioned that such approximate trial functions necessarily result in an overestimate of the free energy of the nematic phase and, as a consequence, the density of the coexisting phases is overestimated. This effect is most clearly seen in the limit $l_P \to \infty$. In that limit, the calculations of Lekkerkerker *et al.* [23] become exact as $L/D \to \infty$. For $l_P = \infty$, the difference between the results of Ref. [23] and the other Onsager-like theories is exclusively due to the fact that the other theories use approximate forms for the orientational distribution functions. In contrast, the difference between our simulations and the exact results of Ref. [23] is not related to the use of approximate trial functions, but to the fact that the results of Ref. [23] apply to the limit $L/D = \infty$, while our simulations have been performed for L/D=40. For polymers with a finite length-to-width ratio, one cannot ignore contributions of virial coefficients higher than the second to the free energy. Frenkel [36] showed that for hard spherocylinders with $L/D = 5$, 10, and 100 in the isotropic phase, the reduced third virial coefficient B_3/B_2^2

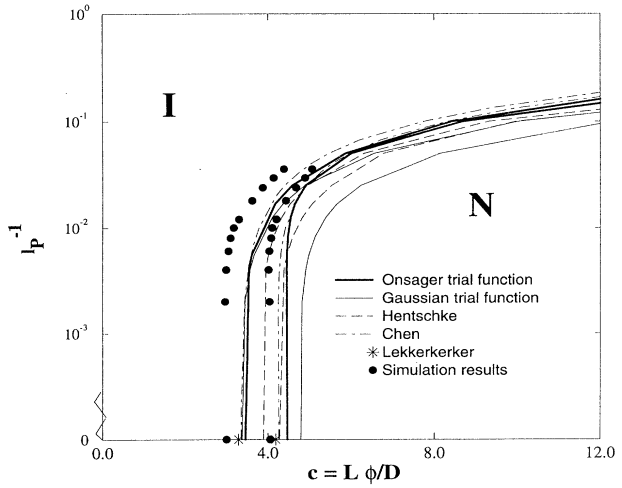

FIG. 2. Phase diagram of a three-dimensional system of semiflexible polymers consisting of ten hard spherocylinders connected to each other.

is equal to, respectively, 0.4194, 0.3133, and 0.0698. In the nematic phase, the contributions of higher virial coefficients is expected to be even larger. In the limiting case of perfectly parallel spherocylinders, the probability of three overlapping particles is not even negligible in the limit $L/D \to \infty$. Another reason why the current theories overestimate the coexisting densities may be related to the approximations made in the calculation of the second virial coefficient of the polymer system. In most theories, the second virial coefficient of a fluid of polymers is approximated by the interaction of a segment of polymer A with a segment of polymer B. In this treatment, the three-and-more segment interactions are completely neglected. One can easily imagine that this approximation is serious, since there is an enhanced probability that the ith segment of polymer A overlaps with segment $i' + 1$ of polymer B, when segment i of polymer A already overlaps with segment i' of polymer B. This effect is caused simply by the fact that segment $i' + 1$ is in the neighborhood of i' due to connectivity and is strongly pronounced as the ℓ/D of the segments is small (in the present case, $\ell/D = 4$).

It should be stressed that not all theories make the assumption that the higher-order virial coefficients can be ignored. Specifically, Hentschke used instead of the second virial approximation a generalization of the Carnahan-Starling equation for hard spheres to the case of spherocylinders, which yields good agreement with Monte Carlo simulations for short spherocylinders [26]. However, Fig. 3 shows clearly that the width of the coexistence region in the simulations is much larger than predicted by Hentschke's theory. Using the Onsager approximation with a Gaussian or Onsager trial function, we observe that the widths of the coexistence regions in the simulations are between these two predictions. However,

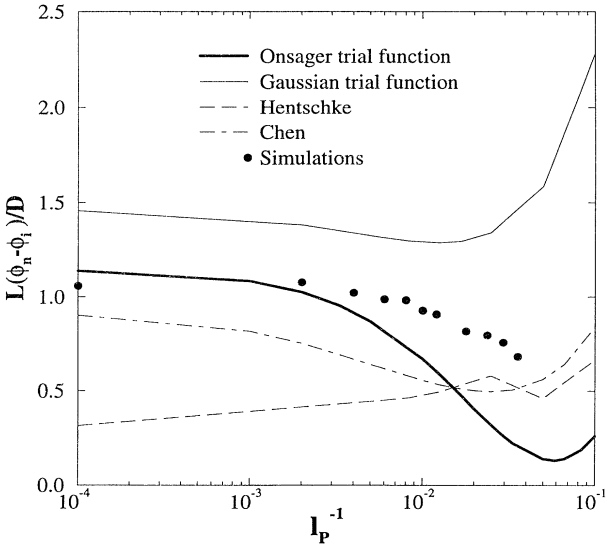

FIG. 3. Width of the coexisting region $(\phi_n - \phi_i)/\phi_i$ vs the inverse persistence length for a three-dimensional system of semiflexible polymers with $L/D = 40$.

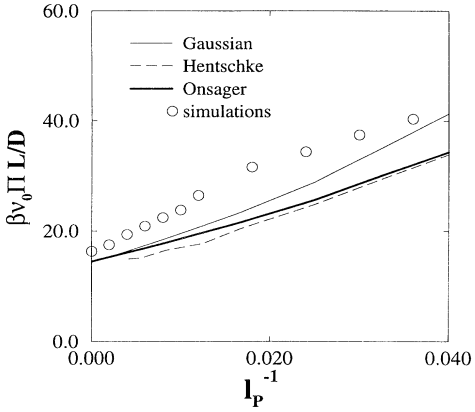

FIG. 4. Pressure vs inverse persistence length for a three-dimensional system of semiflexible polymers with $L/D = 40$.

the width decreases enormously with increasing flexibility when we use the Onsager trial function, whereas the width decreases slightly when a Gaussian trial function is used. Using the Gaussian trial function, Odijk derived a closed expression for the orientational free energy for arbitrary chain length. However, when the Onsager trial

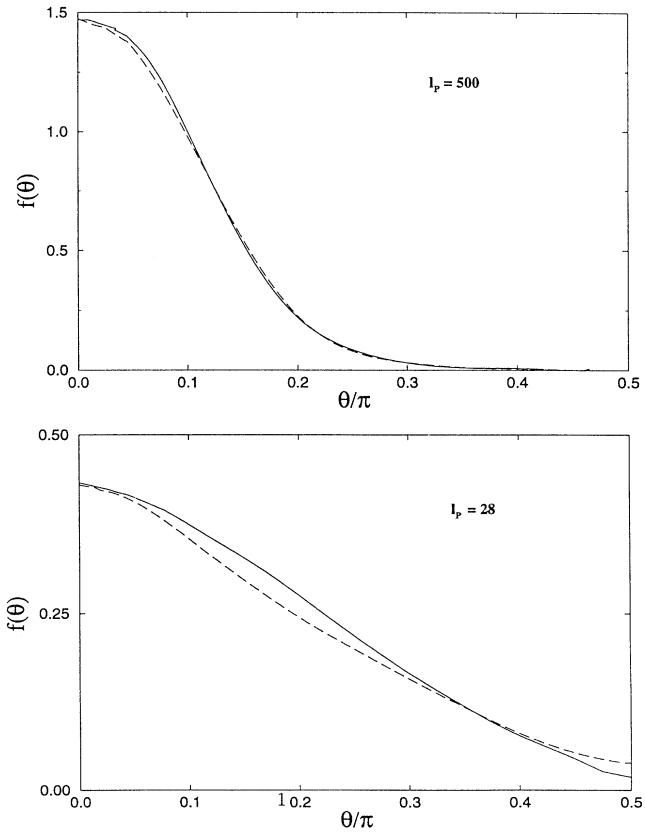

FIG. 5. Orientational distribution function of the segments (solid line) and the end segments of the polymers (dashed line) for persistence length $l_P = 500$ (top) and 28 (bottom) in the nematic phase.

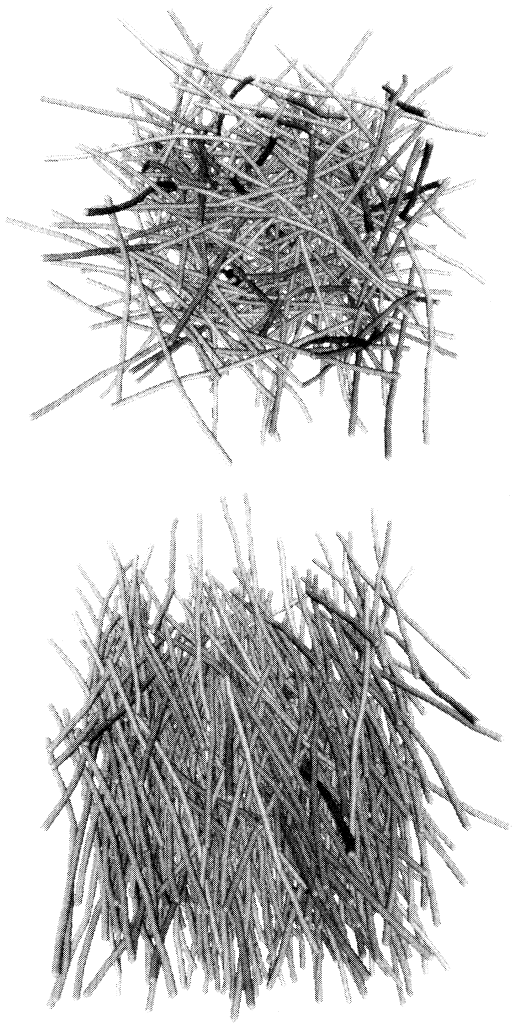

FIG. 6. Typical configurations for a system of semiflexible polymers with persistence length $l_P = 160$ in units of the segment length in the coexisting isotropic (top) and nematic phase (bottom).

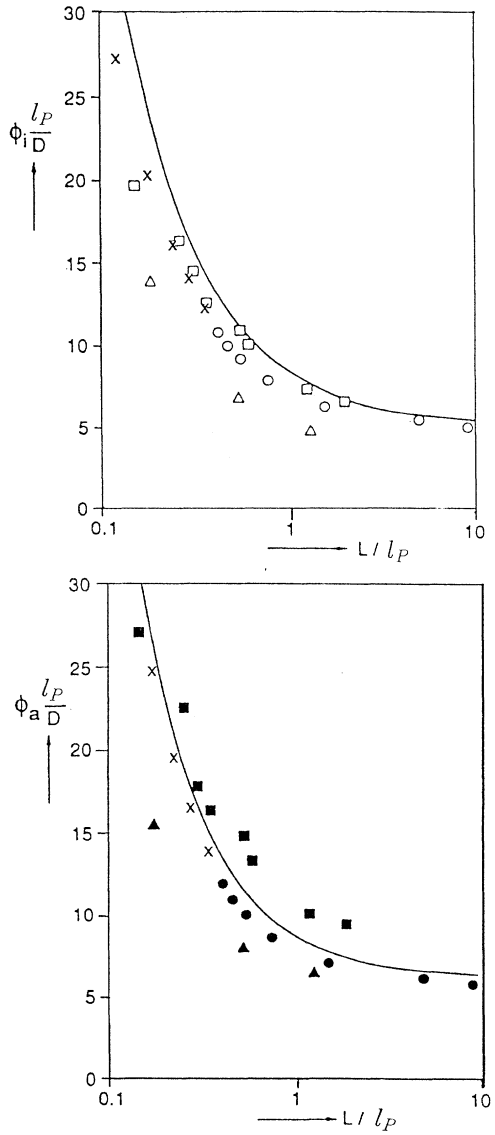

FIG. 7. Scaled isotropic (top) and nematic (bottom) volume fractions at the phase transition vs L/l_P: experimental data for PBLG in dimethylformamide (triangles), PHIC in toluene (circles), Schizophyllan in water (squares), theory using the Onsager trial function (drawn line) and simulation results (crosses).

function was used, we had to interpolate the rod and the semiflexible limit in the form of a Padé approximant in order to obtain a formula valid for arbitrary flexibility. Using the self-consistent method of Chen, we find that our simulation results are higher than these predictions for the width of the coexistence region.

In Fig. 4, we show the pressure at the isotropic-nematic transition, as a function of the inverse persistence length. The pressure in the simulations is systematically higher than predicted by the various theories. In Fig. 5, we show the orientational distribution function for the segments (averaged over all segments) and for the end segments of the polymers for $l_P = 500$ and $l_P = 28$ in the nematic phase. For $l_P = 500$, we find that the orientational distribution function for the segments is similar to the orientational distribution function for the segments. However, for $l_P = 28$, we observe that the orientational distribution function for the end segments is slightly broader than the average orientational distribution. This behavior agrees well with the predictions made by Chen [19]. We also computed the nematic order parameter $S = \langle P_2(\cos\theta)\rangle$ and we find $S = 0.73$ and 0.32 for, respectively, $l_P = 500$ and 28, which should be compared with the values 0.7599 and 0.4897 predicted by Chen. Figure 6 shows typical configurations of the coexisting isotropic and nematic phases for semiflexible polymers with persistence length $l_P = 160$.

Finally, we can compare our simulation results with experimental data. However, there are only a few neutral semiflexible polymers that can be studied well without complications such as aggregation, gelation, and crystal-

lization. Monodisperse systems that have been studied extensively are as follows:

(1) poly(γ-benzyl L-glutamate) (PBLG) in dimethylformamide (L = 16–390 nm, D = 1.6 nm, l_P = 80 nm) [37–41].

(2) poly(n-hexyl isocyanate) (PHIC) in toluene (L = 15-708 nm, D = 1.25 nm, l_P = 40 nm) and in dichloromethane (L = 15–708 nm, D = 1.25 nm, l_P = 20 nm) [42,43].

(3) Schizophyllan in water (L = 49–223 nm, D = 1.7 nm, l_P = 200 nm) [44–47]. In Fig. 7, we show the experimental results for the scaled isotropic and nematic volume fractions versus L/l_P. We observe that our simulation results agree well with the experimental data.

In summary, we have performed Monte Carlo simulations of a three-dimensional system of semiflexible polymers consisting of ten hard spherocylinders connected to each other. Using the Kofke method, we were able to perform simulations along the isotropic-nematic coexistence curve. On the whole, we observe good qualitative agreement with the theoretical predictions and the experimental results. The quantitative differences with the theories are presumably mainly due to the fact that the theories ignore higher-order virial corrections to the free energy.

ACKNOWLEDGMENTS

The work of the FOM Institute is part of the scientific programme of FOM and is supported by the Nederlandse Organisatie voor Wetenschappelijk Onderzoek (NWO). We thank Peter Bolhuis for assistance with the simulations of the hard spherocylinders and René van Roij and Bela Mulder for a critical reading of the manuscript.

[1] G. Vertogen and W.H. de Jeu, *Thermotropic Liquid Crystals, Fundamentals* (Springer-Verlag, Berlin, 1988).
[2] S. Chandrasekhar, *Liquid Crystals* (Cambridge University Press, Cambridge, 1992).
[3] P.G. de Gennes and J. Prost, *The Physics of Liquid Crystals*, 2nd ed. (Clarendon Press, Oxford, 1993).
[4] G.J. Vroege and H.N.W. Lekkerkerker, Rep. Prog. Phys. **55**, 1241 (1992).
[5] P.J. Flory, Proc. R. Soc. London, Ser. A **234**, 60 (1956).
[6] E.A. DiMarzio, J. Chem. Phys. **36**, 1563 (1962).
[7] P.J. Flory and G. Ronca, Mol. Cryst. Liq. Cryst. **54**, 289 (1979).
[8] G. Ronca, J. Polymer. Sci. Pt. B **27**, 1795 (1989).
[9] J.F. Nagle, Proc. R. Soc. London, Ser. A **337**, 569 (1974).
[10] A. Malakis, J. Phys. A **13**, 651 (1980).
[11] A. Baumgärtner, J. Chem. Phys. **84**, 1905 (1986).
[12] A. Kolinsky, J. Skolnick, and R. Yaris, Macromolecules **19**, 2560 (1986).
[13] M.R. Wilson and M.P. Allen, Mol. Phys. **2**, 277 (1993).
[14] A.R. Khokhlov and A.N. Semenov, Physica A **108**, 546 (1981).
[15] A.R. Khokhlov and A.N. Semenov, Physica A **112**, 605 (1982).
[16] T. Odijk, Macromolecules **19**, 2313 (1986).
[17] R. Hentschke, Macromolecules **23**, 1192 (1990).
[18] R. Hentschke and J. Herzfeld, Phys. Rev. A **44**, 1148 (1991).
[19] Z.Y. Chen, Macromolecules **26**, 3419 (1993).
[20] L. Onsager, Ann. N.Y. Acad. Sci. **51**, 627 (1949).
[21] G. Lasher, J. Chem. Phys. **53**, 4141 (1970).
[22] R.F. Kayser and H.J. Raveché, Phys. Rev. A **17**, 2067 (1978).
[23] H.N.W. Lekkerkerker, Ph. Coulon, R. van der Haegen, and R. Deblieck, J. Chem. Phys. **80**, 3427 (1984).
[24] J. Herzfeld, A.E. Berger, and J.W. Wingate, Macromolecules **17**, 1718 (1984).
[25] G.J. Vroege and T. Odijk, Macromolecules **21**, 2848 (1988).
[26] S.J. Lee, J. Chem. Phys. **87**, 4972 (1987).
[27] H. Yamakawa and M. Fujii, J. Chem. Phys. **59**, 6641 (1973).
[28] T. Odijk, Macromolecules **16**, 1340 (1983).
[29] D.A. Kofke, Mol. Phys. **78**, 1331 (1993).
[30] D.A. Kofke, J. Chem. Phys. **98**, 4149 (1993).
[31] W.H. Press, B.P. Flannery, S.A. Teukolsky, and W.T. Vetterling, *Numerical Recipes in Fortran* (Cambridge University Press, New York, 1992).
[32] M.P. Allen and D.J. Tildesley, *Computer Simulations of Liquids* (Clarendon, Oxford, 1987).
[33] M.P. Allen, G.T Evans, D. Frenkel, and B.M. Mulder, *Advances in Chemical Physics* (Wiley and Sons, Inc., Cambridge, 1993), Volume LXXXVI.
[34] D. Frenkel, G.C.A.M. Mooij, and B. Smit, J. Phys. Condens. Matter **4**, 3053 (1992).
[35] M. Dijkstra, D. Frenkel, and H.N.W. Lekkerkerker, Physica A **193**, 374 (1993).
[36] D. Frenkel, J. Phys. Chem. **92**, 5314 (1988) (Erratum); **91**, 4912 (1987).
[37] E.L. Wee and W.G. Miller, J. Phys. Chem. **75**, 1446 (1971).
[38] W.G. Miller, C.C. Wu, E.L. Wee, G.L. Santee, J.H. Rai, and K.G. Goebel, Pure Appl. Chem. **38**, 37 (1974).
[39] P.S. Russo and W.G. Miller, Macromolecules **16**, 1690 (1983).
[40] K. Kubo and K. Ogino, Mol. Cryst. Liq. Cryst. **53**, 207 (1979).
[41] K. Kubo, Mol. Cryst. Liq. Cryst. **74**, 71 (1981).
[42] C. Conio, E. Bianchi, A. Ciferri, and W.R. Krigbaum, Macromolecules **17**, 865 (1984).
[43] T. Itou and A. Teramoto, Macromolecules **21**, 2225 (1988).
[44] K. Van and A. Teramoto, Polym. J. **14**, 999 (1982).
[45] T. Itou and A. Teramoto, Macromolecules **17**, 1419 (1984).
[46] T. Itou and A. Teramoto, Polym. J. **16**, 779 (1984).
[47] T. Kojima, T. Itou, and A. Teramoto, Polym. J. **19**, 1225 (1987).

FIG. 6. Typical configurations for a system of semiflexible polymers with persistence length $l_P = 160$ in units of the segment length in the coexisting isotropic (top) and nematic phase (bottom).